Author Manuscript
Author Manuscript
Author Manuscript
Author Manuscript

HHS Public Access
Author manuscript
NMR Biomed. Author manuscript; available in PMC 2018 March 01.

Published in final edited form as:
NMR Biomed. 2017 March ; 30(3): . doi:10.1002/nbm.3458.

Diffusion MRI in early cancer therapeutic response assessment

C. J. Galbán, **B. A. Hoff**, **T. L. Chenevert**, and **B. D. Ross**[*]
Department of Radiology, Center for Molecular Imaging, University of Michigan, Ann Arbor, MI, USA

Abstract

Imaging biomarkers for the predictive assessment of treatment response in patients with cancer earlier than standard tumor volumetric metrics would provide new opportunities to individualize therapy. Diffusion-weighted MRI (DW-MRI), highly sensitive to microenvironmental alterations at the cellular level, has been evaluated extensively as a technique for the generation of quantitative and early imaging biomarkers of therapeutic response and clinical outcome. First demonstrated in a rodent tumor model, subsequent studies have shown that DW-MRI can be applied to many different solid tumors for the detection of changes in cellularity as measured indirectly by an increase in the apparent diffusion coefficient (ADC) of water molecules within the lesion. The introduction of quantitative DW-MRI into the treatment management of patients with cancer may aid physicians to individualize therapy, thereby minimizing unnecessary systemic toxicity associated with ineffective therapies, saving valuable time, reducing patient care costs and ultimately improving clinical outcome. This review covers the theoretical basis behind the application of DW-MRI to monitor therapeutic response in cancer, the analytical techniques used and the results obtained from various clinical studies that have demonstrated the efficacy of DW-MRI for the prediction of cancer treatment response.

Keywords

review article; cancer treatment response; imaging biomarker; functional diffusion map; diffusion-weighted MRI

INTRODUCTION

Monitoring cancer treatment response

Image-based assessment of cancer treatment response continues to be an active area of research with advances in medical imaging instrumentation providing opportunities to fundamentally change the clinical management of patients with cancer. MRI represents a key modality that has found use in the diagnosis, treatment planning, and assessment of response and recurrence of solid malignancies. By providing high spatial resolution and soft tissue contrast, MRI allows exquisite noninvasive radiographic detection of tumor location, whilst also providing a determination of the tumor number and dimensions.

[*]Correspondence to: B. D. Ross, University of Michigan School of Medicine, Center for Molecular Imaging and Department of Radiology, Biomedical Sciences Research Building, 109 Zina Pitcher Place, Ann Arbor, MI 48109, USA. bdross@umich.edu.

Author Manuscript Author Manuscript Author Manuscript Author Manuscript

Computed tomography and, soon after, MRI have been used since the 1960s to measure gross changes in tumor volume following a therapeutic intervention (1). Although there have been advancements in quantitative imaging techniques, such as diffusion-weighted MRI (DW-MRI), dynamic contrast-enhanced MRI (DCE-MRI) and fluorodeoxyglucose-positron emission tomography (FDG-PET), standard practice for patient management and clinical trials continues to employ anatomical images to assess tumor response to treatment (2–4). The World Health Organization (WHO) and the Response Evaluation Criteria in Solid Tumors (RECIST) have proposed guidelines primarily based on a single linear summation of specific lesions, where monitoring of the morphological changes in tumor volume allows for routine measurements for cancer response assessment. Nevertheless, there continues to be growing concerns regarding the adequacy of these criteria as some treatments, such as molecularly targeted agents, may provide therapeutic benefit without significantly reducing the tumor volume (5–7). These concerns underscore the urgency for the development and implementation of reliable response imaging biomarkers or surrogates that can detect response to treatment earlier than current methodologies (8,9).

GENERAL CONCEPTS IN DIFFUSION

The first diffusion MR sequence was demonstrated in 1965 by Stejskal and Tanner (10) and, by the 1980s, DW-MRI of *in vivo* systems was reported (11–13). Since then, reviews have been generated on the principles and technical aspects of this MR technique, as well as consensus recommendations using diffusion imaging as a response metric for treatment assessment (14–16). Molecular diffusion is the thermally driven random translational motion of molecules in media, which is referred to as ‘Brownian motion’. Key factors that exert their influence on the mobility of a diffusing molecule include medium viscosity, temperature and its molecular mass. Diffusion is not a magnetization-related process such as, for example, T_1 and T_2 magnetization relaxation, which drives conventional MRI contrast. Nevertheless, MRI can be used to noninvasively quantify (image) water diffusion values spatially *in vivo*. This is accomplished in part through the use of magnetic gradients that allow for the ‘encoding’ of initial locations of constituent water molecules in the tissue. Following a brief interval, the same gradients are used to ‘decode’ the molecular locations. For those water molecules in which displacement has occurred during the time interval, decoding will be incomplete, resulting in the loss of signal through spin dephasing. The dephasing amount increases in proportion to the distance translated between encode/decode diffusion gradient pulses. Highly mobile water molecules will have greater attenuation of the signal relative to water in more restricted/cellular tissue environments. The determination of the degree of signal loss at various diffusion gradient settings provides for the ability to calculate molecular mobility in complex systems, such as tumor tissue. However, because tumor tissue is composed of water located in a highly complex microenvironment, the concept of a single diffusion coefficient is not valid and, as such, it is reported as an ‘apparent diffusion coefficient’ (ADC) (13,14). ADC measurements can be used to assess a myriad of properties that impede molecular motions, including cell membrane integrity, cell density, interactions with macromolecules, and processes that enhance mobility via active transport, convective motion and perfusion.

Author Manuscript Author Manuscript Author Manuscript Author Manuscript

The ability of water to sample its surrounding environment is the foundation behind its efficacy as a measure of tumor response to cancer. The thermal, i.e. Brownian, motion of free water at body temperature (~35 °C) is approximately 3×10^{-3} mm^2/s. Clinical DW-MRI sequences typically have a bipolar gradient interval around 50 ms, resulting in a displacement of free water molecules of 30 μm. By applying these motion-sensitive gradients, water molecules can be exploited to sample the microenvironment of biological systems well within the resolution of the MRI sequence. Structures within the solid tumor that are sampled by water molecules may include the tumor cell membranes, organelles, myelin layers and macromolecules, as well as additional cellular and subcellular entities, all of which are on the order of micrometers. Transient association of water with large, slow-moving macromolecules and cell membranes that result in water binding, as well as impediment by membranes and other structures, effectively reduce water mobility to an ADC lower than free water diffusion. The greater the bulk density of structures within a tumor tissue that impede water mobility, the lower the ADC value for that tumor. As such, ADC is considered to be a noninvasive imaging biomarker of cellularity or cell density. However, if two tissues have different ADC values, the lower ADC tissue may not necessarily have the greater number of cells per unit volume. Other factors that make up the microenvironment (e.g. cell size, viscosity, vasculature, extracellular matrix and permeability) also affect water mobility and ADC. Within a given tissue or cell type, ADC is useful as an indicator of the relative cellularity, such as in the evolution of a tumor over time following therapy. Cellular alterations caused by disease or intervention, as well as changes in cellular organization or integrity of cellular elements, are available for study by diffusion imaging.

Water diffusion on the order of cellular distances is measurable in spite of the presence of other much larger physiologic motions. A single-shot echo-planar imaging (EPI) approach (17) is the standard imaging sequence for the acquisition of diffusion-weighted imaging. By acquiring the entire set of echoes for an image within one single scanning period, respiratory bulk tissue motion, which would overwhelm the measurement of molecular motion, is essentially eliminated. By decreasing the acquisition times by a factor of 100, EPI also allows DW-MRI to be incorporated as a standard MRI sequence in clinical scanners to be used in routine clinical scanning protocols. However, images generated by EPI are sensitive to artifacts, such as distortion and signal loss owing to magnetic susceptibility. These limitations aside, EPI is the most commonly used clinical sequence, combined with diffusion sensitization gradient pulses, to perform DW-MRI.

ADC AS A MEASURE OF TUMOR CELLULARITY

It is traditionally viewed that, as cellular density increases, the added tortuosity within the microenvironment reduces water mobility. Figure 1 illustrates the effect of an effective therapeutic agent on the water diffusivity in a solid tumor mass (18). Solid tumors typically have a mean ADC value around 1×10^{-3} mm^2/s (Fig. 1). Following the intervention of a therapeutic agent that results in cell killing (i.e. a decrease in tumor cellularity), the extra-cellular space increases as the intracellular space diminishes (Fig. 1). This results in a shift in the tumor water diffusivity to higher values in therapeutically responsive regions of the tumor. Several groups have reported the inverse relationship between ADC and cellular

Author Manuscript Author Manuscript Author Manuscript Author Manuscript

density (19–22). To aid in the interpretation of these results, a biphasic model relating ADC values to cellularity has been proposed in which two pools of water within the tissue exist: a fast diffusion pool and a slow diffusion pool (23). The slow diffusion pool is proposed to consist of a water layer trapped by electrostatic forces of the cellular membranes and associated cytoskeleton. The fast diffusion pool is thought to belong to a combination of intra- and extracellular compartments which are, however, slower than free water. Both the traditional, i.e. monoexponential, and biphasic diffusion models provide for the rationale that water diffusion will decrease during cell swelling or cell proliferation, and increase during treatment-induced loss of cellular viability or density. Regardless of the underlying mechanism, the fact remains that tumor diffusion values increase as tumor tissue initially progresses from a solid, cellular lesion to an acellular, necrotic tumor during successful cytotoxic therapy. This characteristic of tumor water diffusion values provides a key opportunity to use this biophysical and quantifiable ADC parameter as a sensitive biomarker for the detection of the underlying changes in tumor cytoarchitecture associated with treatment (24).

DIFFUSION IMAGING TO ASSESS TREATMENT RESPONSE

Twenty years of research in preclinical studies have supported the notion that water diffusivity is highly dependent on the tumor microenvironment. This suggests that diffusion MR can be used to noninvasively detect cellular changes associated with treatment-induced cell killing in animal models (19,20,22,25–30). The key findings in many studies are that changes in ADC values precede changes in tumor volume regression, as well as being treatment independent and dose/efficacy dependent. All of this supports the claim that this imaging biomarker may indeed be used as an early surrogate for the assessment of treatment outcome.

Diffusion MRI as a method for therapeutic response assessment in the clinic was first demonstrated in patients with glioma (21). Tumors treated with radiation, with or without chemotherapy, demonstrated an increase in ADC values from baseline. The magnitude of change in ADC values correlated with cellularity in the tumor mass, albeit in a pilot study. Through advances in radiofrequency coil design, parallel imaging and rapid pulse sequencing, diffusion MRI has been demonstrated as a biomarker of treatment response in breast cancer (31–38), liver cancer (39–47), prostate cancer (34,48), rectal cancer (49–57), lymphomas (20,58–63), head and neck cancer (64,65) and metastases (29,33,37,66–72). Results from clinical studies have shown a significant difference in the mean ADC values between patients responding to treatment relative to patients who were determined to be nonresponsive to treatment.

An example of the clinical application of DW-MRI for the assessment of early treatment response was reported in patients with stage II/III breast cancer treated with neoadjuvant chemotherapy (NAC) (73). Presented in Fig. 2 are representative slices of ADC tumor maps from two patients with breast cancer who underwent two cycles of NAC. The first patient revealed an increase in tumor diffusion values (Fig. 2A), indicating that cell killing had occurred with no significant reduction in tumor size (Fig. 2B). Following the second cycle of treatment, a significant decrease in tumor volume was noted. In the second patient with

Author Manuscript Author Manuscript Author Manuscript Author Manuscript

breast cancer, ADC values remained stable over the treatment period and the patient was subsequently classified as non-pathological complete response (non-pCR) (Fig. 2C, D). These data reveal the tremendous potential of DW-MRI for the early monitoring of cancer treatment response.

Although an initial increase in tumor ADC values during treatment is typically associated with cell death, a subsequent decrease in tumor ADC values may occur, indicating tumor regrowth or, possibly, fibrosis. This present understanding is supported by findings in recurrent high-grade gliomas and osteosarcomas, where lower ADC values are observed in viable tumor and higher ADC values in regions of necrosis following treatment (74,75). Thus, ADC values in the context of the determination of the treatment response should probably be limited to early time intervals post-treatment initiation because of the more complex late-stage cellular processes that may complicate interpretation.

Metastatic lesions pose a very distinct problem for the treatment management of patients with cancer with disseminated disease. In many cases, primary tumors that have metastasized will seed osseous regions. Although bone scans using technetium 99m single photon emission computed tomography (Tc99m-SPECT) imaging are standard clinical practice for the diagnosis of metastatic cancer to the bone, RECIST continues to label bony tumors as ‘non-measurable’ because of the complex metabolic state of the bone interacting with the tumor. DW-MRI, with its high soft tissue contrast and resolution, has been shown to be highly sensitive to tumor response to therapy, irrespective of bone turnover. In a preliminary pilot study, Lee *et al.* (29) first demonstrated the utility of DW-MRI for therapeutic response assessment in two patients with metastatic prostate cancer to the bone, which was later validated in a large dataset by Reischauer *et al.* (76).

WHOLE-BODY DIFFUSION-WEIGHTED MRI (WBDW-MRI)

Although the aforementioned studies (29,76) focused only on treatment response in individual tumors, advances in wbDW-MRI may allow for multiple lesions to be monitored simultaneously (77,78). This is illustrated in the work by Horger *et al.* (59), where 20 patients with lymphoma undergoing systemic therapy were monitored using wbDW-MRI. Figure 3 demonstrates the sensitivity of wbDW-MRI for the detection of variations in therapeutic response in a single patient. Multi-focal lesions within the patient were found to have increased ADC values, suggesting that cell killing occurred following treatment, as depicted in these inverted gray-scale images (arrows). In contrast, the large tumor in the pelvic node (arrowhead) revealed a stable ADC value. Through the use of wbDW-MRI, early response assessment can now be obtained over multiple lesions, but at a cost of reduced spatial resolution.

ANOMALIES IN REPORTED DIFFUSION VALUES FOR TUMOR RESPONSE

Most studies have reported that tumor water ADC values typically increase following successful intervention in solid tumors. Although this trend appears to be the norm, there have been cases in which a decrease, rather than an increase, in ADC measurements has been reported to correlate with a positive response (54,79–81). As the tumor mass will

Author Manuscript Author Manuscript Author Manuscript Author Manuscript

respond dynamically throughout the course of fractionated therapies, the timing of the acquired DW-MRI measurement may have an impact on the findings. For example, two studies that investigated the efficacy of DW-MRI on treated rectal cancer (54,80) showed a brief, transient increase in ADC in the first week post-treatment initiation. Subsequently, a decrease in ADC was observed over the next several weeks. Histology confirmed that chemoradiation of rectal carcinoma resulted in increased interstitial fibrosis, which may have had the effect of reducing the ADC values in the tumor regions (54). The authors also drew attention to the fact that regions of obvious necrosis, as observed by MRI within the tumor mass, were not included in the volume of interest prescribed over the tumor mass. Omission of the necrotic regions would bias the measurement to lower ADC values. Therefore, the reported decreased ADC values that correlated with response appear to be primarily related to the timing of the measurement, as well as fibrotic formation following tumor cell death.

SPATIAL HETEROGENEITY IN TUMOR RESPONSE

Spatial heterogeneity in tumor response is a major confounding factor in assigning a single indicator to a patient. A given lesion often contains wide gradations of viable cellularity and necrosis, and the response of tumor subregions to treatment can be nonuniform and dependent on many factors. Histogram analysis of ADC values throughout the tumor is one approach to address heterogeneity (83,84). Although a variety of scalar quantities are derivable from tumor ADC histogram analysis, the magnitude of regional changes may be underestimated by whole-tumor summary statistics in the presence of heterogeneous response patterns. Figure 4 from ref. (85) illustrates the effect of response heterogeneity on the tumor histogram. Using simulated data, the authors demonstrated that uniform changes in tumor ADC values result in a mean ADC value that can detect alterations in tumor ADC values (Fig. 4B). Although other whole-tumor metrics may provide more sensitivity, such as the standard deviation for the case in which regions of the tumor demonstrate increasing and decreasing ADC values from baseline (Fig. 4C), we would need to know a priori the most appropriate measure. A more comprehensive evaluation has been performed on the efficacy of histogram-based measures for therapeutic response assessment using MRI-derived blood volume maps in patients with glioma (86). Although not performed using DW-MRI acquired parameters, the study observed negligible effectiveness of a variety of whole-tumor quantitative metrics for the detection of tumor response at both 1 and 3 weeks post-treatment initiation.

An alternative image processing approach has been developed to quantify and spatially map the intrinsic treatment-associated heterogeneity of diffusion values within a tumor. This technique is referred to as ‘functional diffusion mapping’ (fDM) (87). A key element of fDM is the spatial registration of baseline and follow-up three-dimensional quantitative diffusion maps (i.e. ADC) into a single geometrical space. Further reading on the registration techniques and limitations for therapeutic response assessment is provided in refs. (85,88,89). Once registered, diffusion changes are measured on a voxel-by-voxel basis from spatially aligned pre-treatment and post-treatment initiation ADC maps. Tumor voxels are then classified by their extent of change in ADC. Although fDM was initially evaluated in patients with glioma (87,90–93), this technique has been applied to other tumor types

Author Manuscript Author Manuscript Author Manuscript Author Manuscript

(29,65,76,85). Figure 5 shows fDMs [also referred to as parametric response mapping (PRM_{ADC})] with corresponding scatter plots from patients with head and neck squamous cell carcinoma (HNSCC) diagnosed as complete response (CR) (Fig. 5A) and partial response (PR) (Fig. 5B) following therapy. By analysis of the diffusion maps using fDM, heterogeneity in tumor response can be visualized, with red regions denoting response (i.e. increase in ADC from baseline) *versus* stable and decreased ADC regions depicted as green and blue, respectively. As demonstrated in a variety of tumor types, large regions of increased ADC from baseline (i.e. red voxels) were strongly correlated with treatment response, irrespective of the presence of tumor regions with stable or decreasing ADC values.

STANDARDIZATION AND REPEATABILITY OF ADC MEASUREMENTS

As discussed in this review, the biophysical premise and technical feasibility have allowed quantitative DW-MRI to become a clinically viable technique. Nevertheless, for this imaging protocol to become routine in the management of patients and clinical trials, there is a need to standardize DW-MRI acquisition schemes to account for intra and inter-vendor instrument variability (94). In an effort to bring uniformity throughout the various MRI systems, phantoms have been developed to confirm quantitative agreement across platforms. The ideal phantom must be stable throughout the imaging sequences and provide meaningful ADC measurements consistent with biological systems. As a result of the complexity of water diffusion in living tissue, the development of a phantom that is both stable and mimics all tissue properties has its difficulties. Simple fluid-based test objects are the preferred approach to phantom development using fluids that are thermally stable, readily available and safe when properly handled (95,96). In a study by Tofts *et al.* (97), the diffusion coefficients of 15 organic liquids were evaluated and found to stably provide repeatable ADC measurements within the relevant range of biological systems [$(0.36–2.6) \times 10^{-3}$ mm^2/s]. In 2011, Chenevert *et al.* (98) reported a temperature-controlled phantom using water cooled to near freezing. This phantom consisted of liquid water jacketed with ice water, such that the inner chamber was cooled to ~0 °C. Although water diffusivity is highly sensitive to temperature (99), jacketing the liquid water with ice allowed a stable environment with temperatures maintained for up to 4 h and a reliable, biologically relevant ADC value ($\sim 1 \times 10^{-3}$ mm^2/s). The availability of stable and reproducible phantoms has allowed multi-center studies to be performed, demonstrating the repeatability of quantitative DW-MRI across platforms (100,101).

In the absence of a standard DW-MRI protocol, investigators of clinical trials are employing strategies to contend with intra-instrument variability. Affectionately referred to as the ‘coffee-break exam’, this approach acquires repeat DW-MRI examinations, minutes to hours apart, to ascertain the variability in the ADC measurement prior to therapeutic intervention. The motivation of this strategy is to characterize the noise associated with the ADC measurement for a given patient and platform in the absence of disease- or treatment-related changes in tumor physiology and anatomy. Various studies, just to name a few, have reported stable quantitative DW-MRI measurements in HNSCCs (64), hepatocellular carcinoma (102), malignant lung lesions (103), rectal cancer (104) and primary breast cancer (105). Until uniformity in DW-MRI protocols between vendors, instruments and sites is obtained,

Author Manuscript Author Manuscript Author Manuscript Author Manuscript

the strategy of repeat examinations prior to therapeutic intervention will help to elevate some of the variability in the ADC measurement within a given instrument.

FUTURE DIRECTIONS

The studies presented here support the use of DW-MRI as an early surrogate biomarker for tumor response assessment. In a growing body of literature, changes in tumor water diffusion values have been reported to correlate with response to therapy, despite the diverse set of tumor types, MRI manufacturers and magnetic field strengths used to collect the data, together with the varying approaches used to analyse the datasets (Figure 6, Table 1). Taken together, this reveals the overall robustness of DW-MRI for oncological treatment assessment. Clinical cancer studies on the efficacy of DW-MRI as a surrogate imaging biomarker of the tumor treatment response have demonstrated that treatment-induced cell death can be detected in responding tumors as an increased ADC value in these regions. As a result of variability in DW-MRI acquisition and analytical post-processing protocols, efforts have solidified in the publication of a consensus paper to provide for standardization across institutions (16). In addition, temperature-controlled phantoms have recently been developed to facilitate multi-center DW-MRI clinical trials (100,101). These standards are needed for data acquisition, post-image processing, timing of evaluation and the method used to generate the quantifiable metric used to report treatment response. Although the momentum for the use of DW-MRI in the context of tumor response assessment is continuing to grow, validation of DW-MRI as a surrogate imaging biomarker of response will require a large, prospective, multi-institutional trial performed in a standardized fashion between sites. Analysis of the data could also be useful for the validation of the image post-processing software and for regulatory approval as a device. Having a Food and Drug Administration (FDA)- or European-approved software package would provide additional momentum for enhancing the probability that DW-MRI will ultimately be incorporated into routine clinical practice for the management of patients with cancer. Future opportunities in employing DW-MRI in the clinical management of patients with cancer may include adaptive therapy protocols based on intra-therapy evaluation of early ADC changes during fractionated dosage schedules, allowing for the modification of interventions and for the quantification of multi-focal disease response using wbDW-MRI (78). Finally, the recent emergence of anticancer immunotherapies raises an urgent need for the establishment of radiological metrics for assessment of the response to such experimental interventions (106–108). Further efforts investigating advanced imaging techniques, such as DW-MRI, are needed to delineate its ability to provide meaningful insights into treatment responsiveness in order for it to have a successful impact on clinical decision making.

Supplementary Material

Refer to Web version on PubMed Central for supplementary material.

Acknowledgments

Funding support for this work was provided by the National Institutes of Health grants P01CA085878 and U01CA166104.

Author Manuscript Author Manuscript Author Manuscript Author Manuscript

Abbreviations used

ADC	apparent diffusion coefficient
CR	complete response
DCE-MRI	dynamic contrast-enhanced MRI
DW-MRI	diffusion-weighted MRI
EPI	echo-planar imaging
FDG-PET	fluorodeoxyglucose-positron emission tomography
FDM	functional diffusion map
HNSCC	head and neck squamous cell carcinoma
NAC	neoadjuvant chemotherapy
PCR	pathological complete response
PR	partial response
PRM	parametric response mapping
RECIST	Response Evaluation Criteria in Solid Tumors
Tc99m-SPECT	technetium 99m single photon emission computed tomography
wbDW-MRI	whole-body diffusion-weighted MRI
WHO	World Health Organization

References

1. Gehan EA, et al. Historical and methodological developments in clinical trials at the National Cancer Institute. Stat Med. 1990; 9(8):871–80. discussion 903–906. [PubMed: 2218190]
2. Eisenhauer EA, et al. New response evaluation criteria in solid tumours: revised RECIST guideline (version 1.1). Eur J Cancer. 2009; 45(2):228–47. [PubMed: 19097774]
3. Wen PY, et al. Updated response assessment criteria for high-grade gliomas: response assessment in neuro-oncology working group. J Clin Oncol. 2010; 28(11):1963–72. [PubMed: 20231676]
4. World Health Organization (WHO). WHO Handbook for Reporting Results of Cancer Treatment. Geneva: WHO; 1979.
5. Jaffe CC. Measures of response: RECIST, WHO, and new alternatives. J Clin Oncol. 2006; 24(20): 3245–51. [PubMed: 16829648]
6. Choi H, et al. CT evaluation of the response of gastrointestinal stromal tumors after imatinib mesylate treatment: a quantitative analysis correlated with FDG PET findings. Am J Roentgenol. 2004; 183(6):1619–28. [PubMed: 15547201]
7. Strumberg D, et al. Phase I clinical and pharmacokinetic study of the novel Raf kinase and vascular endothelial growth factor receptor inhibitor BAY 43-9006 in patients with advanced refractory solid tumors. J Clin Oncol. 2005; 23(5):965–72. [PubMed: 15613696]

Author Manuscript

Author Manuscript

Author Manuscript

Author Manuscript

8. Barrington SF, et al. Role of imaging in the staging and response assessment of lymphoma: consensus of the International Conference on Malignant Lymphomas Imaging Working Group. J Clin Oncol. 2014; 32(27):3048–58. [PubMed: 25113771]
9. Cheson BD, et al. Recommendations for initial evaluation, staging, and response assessment of Hodgkin and non-Hodgkin lymphoma: the Lugano classification. J Clin Oncol. 2014; 32(27):3059–68. [PubMed: 25113753]
10. Stejskal E, et al. Spin diffusion measurements: spin echoes in the presence of a time-dependent field gradient. J Chem Phys. 1965; 42(1):288–92.
11. Thomsen C, et al. In vivo measurement of water self diffusion in the human brain by magnetic resonance imaging. Acta Radiol. 1987; 28(3):353–61. [PubMed: 2958045]
12. Merboldt KD, et al. MRI of “diffusion” in the human brain: new results using a modified CE-FAST sequence. Magn Reson Med. 1989; 9(3):423–9. [PubMed: 2710008]
13. Le Bihan D, et al. Separation of diffusion and perfusion in intravoxel incoherent motion MR imaging. Radiology. 1988; 168(2):497–505. [PubMed: 3393671]
14. Le Bihan D. Molecular diffusion nuclear magnetic resonance imaging. Magn Reson Q. 1991; 7(1): 1–30. [PubMed: 2043461]
15. Bammer R. Basic principles of diffusion-weighted imaging. Eur J Radiol. 2003; 45(3):169–84. [PubMed: 12595101]
16. Padhani AR, et al. Diffusion-weighted magnetic resonance imaging as a cancer biomarker: consensus and recommendations. Neoplasia. 2009; 11(2):102–25. [PubMed: 19186405]
17. Edelman RR, et al. Echo-planar MR imaging. Radiology. 1994; 192(3):600–12. [PubMed: 8058920]
18. Hamstra DA, et al. Diffusion magnetic resonance imaging: a bio-marker for treatment response in oncology. J Clin Oncol. 2007; 25(26):4104–9. [PubMed: 17827460]
19. Lyng H, et al. Measurement of cell density and necrotic fraction in human melanoma xenografts by diffusion weighted magnetic resonance imaging. Magn Reson Med. 2000; 43(6):828–36. [PubMed: 10861877]
20. Guo AC, et al. Lymphomas and high-grade astrocytomas: comparison of water diffusibility and histologic characteristics. Radiology. 2002; 224(1):177–83. [PubMed: 12091680]
21. Chenevert TL, et al. Diffusion magnetic resonance imaging: an early surrogate marker of therapeutic efficacy in brain tumors. J Natl Cancer Inst. 2000; 92(24):2029–36. [PubMed: 11121466]
22. Chenevert TL, et al. Monitoring early response of experimental brain tumors to therapy using diffusion magnetic resonance imaging. Clin Cancer Res. 1997; 3(9):1457–66. [PubMed: 9815831]
23. Le Bihan D. The ’wet mind’: water and functional neuroimaging. Phys Med Biol. 2007; 52(7):R57–90. [PubMed: 17374909]
24. Chenevert TL, et al. Diffusion imaging: insight to cell status and cytoarchitecture. Neuroimaging Clin N Am. 2006; 16(4):619–32. viii–ix. [PubMed: 17148023]
25. Ross BD, et al. Evaluation of cancer therapy using diffusion magnetic resonance imaging. Mol Cancer Ther. 2003; 2(6):581–7. [PubMed: 12813138]
26. Huang CF, et al. Diffusion magnetic resonance imaging as an evaluation of the response of brain metastases treated by stereotactic radiosurgery. Surg Neurol. 2008; 69(1):62–8. discussion 68. [PubMed: 18054618]
27. Lee KC, et al. Noninvasive molecular imaging sheds light on the synergy between 5-fluorouracil and TRAIL/Apo2L for cancer therapy. Clin Cancer Res. 2007; 13(6):1839–46. [PubMed: 17363540]
28. Lee KC, et al. Dynamic imaging of emerging resistance during cancer therapy. Cancer Res. 2006; 66(9):4687–892. [PubMed: 16651420]
29. Lee KC, et al. A feasibility study evaluating the functional diffusion map as a predictive imaging biomarker for detection of treatment response in a patient with metastatic prostate cancer to the bone. Neoplasia. 2007; 9(12):1003–11. [PubMed: 18084607]
30. Hamstra DA, et al. The use of ^{19}F spectroscopy and diffusion-weighted MRI to evaluate differences in gene-dependent enzyme prodrug therapies. Mol. Ther. 2004; 10(5):916–28.

Author Manuscript Author Manuscript Author Manuscript Author Manuscript

31. Bufi E, et al. Effect of breast cancer phenotype on diagnostic performance of MRI in the prediction to response to neoadjuvant treatment. Eur J Radiol. 2014; 83(9):1631–8. [PubMed: 24938669]
32. Chinnaiyan AM, et al. Combined effect of tumor necrosis factor-related apoptosis-inducing ligand and ionizing radiation in breast cancer therapy. Proc Natl Acad Sci USA. 2000; 97(4):1754–9. [PubMed: 10677530]
33. Gaeta M, et al. Use of diffusion-weighted, intravoxel incoherent motion, and dynamic contrast-enhanced MR imaging in the assessment of response to radiotherapy of lytic bone metastases from breast cancer. Acad Radiol. 2014; 21(10):1286–93. [PubMed: 25088834]
34. Liu L, et al. Diffusion-weighted MRI in early assessment of tumour response to radiotherapy in high-risk prostate cancer. Br J Radiol. 2014; 87(1043):20140359. [PubMed: 25162831]
35. Pickles MD, et al. Diffusion changes precede size reduction in neo-adjuvant treatment of breast cancer. Magn Reson Imaging. 2006; 24(7):843–7. [PubMed: 16916701]
36. Sharma U, et al. Longitudinal study of the assessment by MRI and diffusion-weighted imaging of tumor response in patients with locally advanced breast cancer undergoing neoadjuvant chemotherapy. NMR Biomed. 2009; 22(1):104–13. [PubMed: 18384182]
37. Theilmann RJ, et al. Changes in water mobility measured by diffusion MRI predict response of metastatic breast cancer to chemotherapy. Neoplasia. 2004; 6(6):831–7. [PubMed: 15720810]
38. Yankeelov TE, et al. Integration of quantitative DCE-MRI and ADC mapping to monitor treatment response in human breast cancer: initial results. Magn Reson Imaging. 2007; 25(1):1–13. [PubMed: 17222711]
39. Bonekamp S, et al. Hepatocellular carcinoma: response to TACE assessed with semiautomated volumetric and functional analysis of diffusion-weighted and contrast-enhanced MR imaging data. Radiology. 2011; 260(3):752–61. [PubMed: 21771960]
40. Corona-Villalobos CP, et al. Volumetric assessment of tumour response using functional MR imaging in patients with hepatocellular carcinoma treated with a combination of doxorubicin-eluting beads and sorafenib. Eur Radiol. 2014; XX:XX–XX.
41. Deng J, et al. Diffusion-weighted MR imaging for determination of hepatocellular carcinoma response to yttrium-90 radioembolization. J Vasc Interv Radiol. 2006; 17(7):1195–200. [PubMed: 16868174]
42. Kamel IR, et al. The role of functional MR imaging in the assessment of tumor response after chemoembolization in patients with hepatocellular carcinoma. J Vasc Intervent Radiol. 2006; 17(3):505–12.
43. Kamel IR, et al. Unresectable hepatocellular carcinoma: serial early vascular and cellular changes after transarterial chemoembolization as detected with MR imaging. Radiology. 2009; 250(2):466–73. [PubMed: 19188315]
44. Kamel IR, et al. Functional MR imaging assessment of tumor response after ^{90}Y microsphere treatment in patients with unresectable hepatocellular carcinoma. J. Vasc. Intervent. Radiol. 2007; 18(1 Pt 1):49–56.
45. Mannelli L, et al. Serial diffusion-weighted MRI in patients with hepatocellular carcinoma: prediction and assessment of response to transarterial chemoembolization. Preliminary experience. Eur J Radiol. 2013; 82(4):577–82. [PubMed: 23246330]
46. Rhee TK, et al. Tumor response after yttrium-90 radioembolization for hepatocellular carcinoma: comparison of diffusion-weighted functional MR imaging with anatomic MR imaging. J Vasc Intervent Radiol. 2008; 19(8):1180–6.
47. Yu JS, et al. Added value of diffusion-weighted imaging in the MRI assessment of perilesional tumor recurrence after chemoembolization of hepatocellular carcinomas. J Magn Reson Imaging. 2009; 30(1):153–60. [PubMed: 19557734]
48. Zelhof B, et al. Correlation of diffusion-weighted magnetic resonance data with cellularity in prostate cancer. BJU Int. 2008; XX:XX–XX.
49. Barbaro B, et al. Diffusion-weighted magnetic resonance imaging in monitoring rectal cancer response to neoadjuvant chemoradiotherapy. Int J Radiat Oncol Biol Phys. 2012; 83(2):594–9. [PubMed: 22099033]

Author Manuscript Author Manuscript Author Manuscript Author Manuscript

50. Birlik B, et al. Diffusion-weighted MRI and MR-volumetry in the evaluation of tumor response after preoperative chemoradiotherapy in patients with locally advanced rectal cancer. Magn Reson Imaging. 2014; XX:XX–XX.
51. Carbone SF, et al. Diffusion-weighted MR volumetry for assessing the response of rectal cancer to combined radiation therapy with chemotherapy. Radiology. 2012; 263(1):311. [PubMed: 22438457]
52. Carbone SF, et al. Assessment of response to chemoradiation therapy in rectal cancer using MR volumetry based on diffusion-weighted data sets: a preliminary report. Radiol Med. 2012; 117(7): 1112–24. [PubMed: 22580810]
53. Genovesi D, et al. Diffusion-weighted magnetic resonance for prediction of response after neoadjuvant chemoradiation therapy for locally advanced rectal cancer: preliminary results of a monoinstitutional prospective study. Eur J Surg Oncol. 2013; 39(10):1071–8. [PubMed: 23953231]
54. Hein PA, et al. Diffusion-weighted magnetic resonance imaging for monitoring diffusion changes in rectal carcinoma during combined, preoperative chemoradiation: preliminary results of a prospective study. Eur J Radiol. 2003; 45(3):214–22. [PubMed: 12595106]
55. Ippolito D, et al. Response to neoadjuvant therapy in locally advanced rectal cancer: assessment with diffusion-weighted MR imaging and ^{18}FDG PET/CT. Abdom Imaging. 2012; 37(6):1032–40. [PubMed: 22270580]
56. Kim SH, et al. Locally advanced rectal cancer: added value of diffusion-weighted MR imaging in the evaluation of tumor response to neoadjuvant chemo- and radiation therapy. Radiology. 2009; 253(1):116–25. [PubMed: 19789256]
57. Kim SH, et al. Apparent diffusion coefficient for lymph node characterization after chemoradiation therapy for locally advanced rectal cancer. Acta Radiol. 2014; XX:XX–XX.
58. De Paepe K, et al. Whole-body diffusion-weighted magnetic resonance imaging at 3 Tesla for early assessment of treatment response in non-Hodgkin lymphoma: a pilot study. Cancer Imaging. 2013; 13:53–62. [PubMed: 23466737]
59. Horger M, et al. Very early indicators of response to systemic therapy in lymphoma patients based on alterations in water diffusivity—a preliminary experience in 20 patients undergoing whole-body diffusion-weighted imaging. Eur J Radiol. 2014; 83(9):1655–64. [PubMed: 24972451]
60. Montoro J, et al. Comparison of whole-body diffusion-weighted magnetic resonance and FDG-PET/CT in the assessment of Hodgkin's lymphoma for staging and treatment response. Ecancermedicalscience. 2014; 8:429. [PubMed: 24963346]
61. Prat MC, et al. Ocular adnexal lymphoma: monitoring response to therapy with diffusion-weighted imaging. Ophth Plast Reconstruct Surg. 2013; 29(6):424–7.
62. Siegel MJ, et al. Diffusion-weighted MRI for staging and evaluation of response in diffuse large B-cell lymphoma: a pilot study. NMR Biomed. 2014; 27(6):681–91. [PubMed: 24700565]
63. Tsuji K, et al. Evaluation of staging and early response to chemotherapy with whole-body diffusion-weighted MRI in malignant lymphoma patients: a comparison with FDG-PET/CT. J Magn Reson Imaging. 2014; XX:XX–XX.
64. Ding Y, et al. TU-F-CAMPUS-I-01: head and neck squamous cell carcinoma: short-term repeatability of apparent diffusion coefficient and intravoxel incoherent motion parameters at 3.0T. Med Phys. 2015; 42(6):3646.
65. Galban CJ, et al. A feasibility study of parametric response map analysis of diffusion-weighted magnetic resonance imaging scans of head and neck cancer patients for providing early detection of therapeutic efficacy. Transl Oncol. 2009; 2(3):184–90. [PubMed: 19701503]
66. Blackledge MD, et al. Assessment of treatment response by total tumor volume and global apparent diffusion coefficient using diffusion-weighted MRI in patients with metastatic bone disease: a feasibility study. PloS One. 2014; 9(4):e91779. [PubMed: 24710083]
67. Byun WM, et al. Diffusion-weighted MR imaging of metastatic disease of the spine: assessment of response to therapy. Am J Neuroradiol. 2002; 23(6):906–12. [PubMed: 12063214]
68. Cui Y, et al. Apparent diffusion coefficient: potential imaging bio-marker for prediction and early detection of response to chemotherapy in hepatic metastases. Radiology. 2008; 248(3):894–900. [PubMed: 18710982]

Author Manuscript Author Manuscript Author Manuscript Author Manuscript

69. Kukuk GM, et al. Diffusion-weighted imaging with acquisition of three b-values for response evaluation of neuroendocrine liver metastases undergoing selective internal radiotherapy. Eur Radiol. 2014; 24(2):267–76. [PubMed: 24081644]

70. Marugami N, et al. Early detection of therapeutic response to hepatic arterial infusion chemotherapy of liver metastases from colorectal cancer using diffusion-weighted MR imaging. Cardiovasc Intervent Radiol. 2009; 32(4):638–46. [PubMed: 19238482]

71. Mungai F, et al. Diffusion-weighted magnetic resonance imaging in the prediction and assessment of chemotherapy outcome in liver metastases. Radiol Med. 2014; 119(8):625–33. [PubMed: 24408046]

72. Schmidt S, et al. Diffusion-weighted magnetic resonance imaging in metastatic gastrointestinal stromal tumor (GIST): a pilot study on the assessment of treatment response in comparison with ^{18}F-FDG PET/CT. Acta Radiol. 2013; 54(8):837–42. [PubMed: 23761549]

73. Li X, et al. Multiparametric magnetic resonance imaging for predicting pathological response after the first cycle of neoadjuvant chemotherapy in breast cancer. Invest Radiol. 2014; XX:XX–XX.

74. Uhl M, et al. Osteosarcoma: preliminary results of in vivo assessment of tumor necrosis after chemotherapy with diffusion- and perfusion-weighted magnetic resonance imaging. Invest Radiol. 2006; 41(8):618–23. [PubMed: 16829744]

75. Hein PA, et al. Diffusion-weighted imaging in the follow-up of treated high-grade gliomas: tumor recurrence versus radiation injury. Am J Neuroradiol. 2004; 25(2):201–9. [PubMed: 14970018]

76. Reischauer C, et al. Bone metastases from prostate cancer: assessing treatment response by using diffusion-weighted imaging and functional diffusion maps—initial observations. Radiology. 2010; 257(2):523–31. [PubMed: 20829534]

77. Takahara T, et al. Diffusion weighted whole body imaging with background body signal suppression (DWIBS): technical improvement using free breathing, STIR and high resolution 3D display. Radiat Med. 2004; 22(4):275–82. [PubMed: 15468951]

78. Kwee TC, et al. Diffusion-weighted whole-body imaging with background body signal suppression (DWIBS): features and potential applications in oncology. Eur Radiol. 2008; 18(9):1937–52. [PubMed: 18446344]

79. Dzik-Jurasz A, et al. Diffusion MRI for prediction of response of rectal cancer to chemoradiation. Lancet. 2002; 360(9329):307–8. [PubMed: 12147376]

80. Kremser C, et al. Preliminary results on the influence of chemoradiation on apparent diffusion coefficients of primary rectal carcinoma measured by magnetic resonance imaging. Strahlenther Onkol. 2003; 179(9):641–9. [PubMed: 14628131]

81. Jacobs MA, et al. Uterine fibroids: diffusion-weighted MR imaging for monitoring therapy with focused ultrasound surgery—preliminary study. Radiology. 2005; 236(1):196–203. [PubMed: 15987974]

82. Aliu SO, et al. MRI methods for evaluating the effects of tyrosine kinase inhibitor administration used to enhance chemotherapy efficiency in a breast tumor xenograft model. J Magn Reson Imaging. 2009; 29(5):1071–9. [PubMed: 19388114]

83. Just N. Improving tumour heterogeneity MRI assessment with histograms. Br J Cancer. 2014; 111(12):2205–13. [PubMed: 25268373]

84. Woo S, et al. Histogram analysis of apparent diffusion coefficient map of diffusion-weighted MRI in endometrial cancer: a preliminary correlation study with histological grade. Acta Radiol. 2014; 55(10):1270–7. [PubMed: 24316663]

85. Boes JL, et al. Image registration for quantitative parametric response mapping of cancer treatment response. Transl Oncol. 2014; 7(1):101–10. [PubMed: 24772213]

86. Lemasson B, et al. Impact of perfusion map analysis on early survival prediction accuracy in glioma patients. Transl Oncol. 2013; 6(6):766–74. [PubMed: 24466380]

87. Moffat BA, et al. Functional diffusion map: a noninvasive MRI bio-marker for early stratification of clinical brain tumor response. Proc Natl Acad Sci USA. 2005; 102(15):5524–9. [PubMed: 15805192]

88. Li X, et al. A nonrigid registration algorithm for longitudinal breast MR images and the analysis of breast tumor response. Magn Reson Imaging. 2009; 27(9):1258–70. [PubMed: 19525078]

Author Manuscript Author Manuscript Author Manuscript Author Manuscript

89. Li X, et al. Validation of an algorithm for the nonrigid registration of longitudinal breast MR images using realistic phantoms. Med Phys. 2010; 37(6):2541–52. [PubMed: 20632566]

90. Ellingson BM, et al. Quantitative probabilistic functional diffusion mapping in newly diagnosed glioblastoma treated with radiochemotherapy. Neuro-oncology. 2013; 15(3):382–90. [PubMed: 23275575]

91. Ellingson BM, et al. Functional diffusion maps (fDMs) evaluated before and after radiochemotherapy predict progression-free and overall survival in newly diagnosed glioblastoma. Neuro-oncology. 2012; 14(3):333–43. [PubMed: 22270220]

92. Hamstra DA, et al. Evaluation of the functional diffusion map as an early biomarker of time-to-progression and overall survival in high-grade glioma. Proc Natl Acad Sci USA. 2005; 102(46):16, 759–64.

93. Hamstra DA, et al. Functional diffusion map as an early imaging bio-marker for high-grade glioma: correlation with conventional radiologic response and overall survival. J Clin Oncol. 2008; 26(20):3387–94. [PubMed: 18541899]

94. Padhani AR, et al. Diffusion-weighted magnetic resonance imaging as a cancer biomarker: consensus and recommendations. Neoplasia. 2009; 11(2):102–25. [PubMed: 19186405]

95. Delakis I, et al. Developing a quality control protocol for diffusion imaging on a clinical MRI system. Phys Med Biol. 2004; 49(8):1409–22. [PubMed: 15152682]

96. Laubach HJ, et al. A phantom for diffusion-weighted imaging of acute stroke. J Magn Reson Imaging. 1998; 8(6):1349–54. [PubMed: 9848751]

97. Tofts PS, et al. Test liquids for quantitative MRI measurements of self-diffusion coefficient in vivo. Magn Reson Med. 2000; 43(3):368–74. [PubMed: 10725879]

98. Chenevert TL, et al. Diffusion coefficient measurement using a temperature-controlled fluid for quality control in multicenter studies. J Magn Reson Imaging. 2011; 34(4):983–7. [PubMed: 21928310]

99. Simpson JH, et al. Diffusion and nuclear spin relaxation in water. Phys Rev. 1958; 111:1201–2.

100. Belli G, et al. Quality assurance multicenter comparison of different MR scanners for quantitative diffusion-weighted imaging. J Magn Reson Imaging. 2015; XX:XX–XX.

101. Malyarenko D, et al. Multi-system repeatability and reproducibility of apparent diffusion coefficient measurement using an ice–water phantom. J Magn Reson Imaging. 2013; 37(5):1238–46. [PubMed: 23023785]

102. Kakite S, et al. Hepatocellular carcinoma: short-term reproducibility of apparent diffusion coefficient and intravoxel incoherent motion parameters at 3.0T. J Magn Reson Imaging. 2015; 41(1):149–56. [PubMed: 24415565]

103. Bernardin L, et al. Diffusion-weighted magnetic resonance imaging for assessment of lung lesions: repeatability of the apparent diffusion coefficient measurement. Eur Radiol. 2014; 24(2): 502–11. [PubMed: 24275802]

104. Intven M, et al. Repeatability of diffusion-weighted imaging in rectal cancer. J Magn Reson Imaging. 2014; 40(1):146–50. [PubMed: 24127172]

105. Galban CJ, et al. Multi-site clinical evaluation of DW-MRI as a treatment response metric for breast cancer patients undergoing neo-adjuvant chemotherapy. PloS One. 2015; 10(3):e0122151. [PubMed: 25816249]

106. Heo S, et al. A case of posterior reversible encephalopathy syndrome in a child with myelodysplastic syndrome following allogenic bone marrow transplantation. Pediatr Hematol Oncol. 2010; 27(1):59–64. [PubMed: 20121556]

107. Huang RY, et al. Pitfalls in the neuroimaging of glioblastoma in the era of antiangiogenic and immuno/targeted therapy – detecting illusive disease, defining response. Frontiers Neurol. 2015; 6:33.

108. Rygh CB, et al. Dynamic contrast enhanced MRI detects early response to adoptive NK cellular immunotherapy targeting the NG2 proteoglycan in a rat model of glioblastoma. PloS One. 2014; 9(9):e108414. [PubMed: 25268630]

109. McDonald K, et al. Patterns of shift in ADC distributions in abdominal tumours during chemotherapy-feasibility study. Pediatr Radiol. 2011; 41(1):99–106. [PubMed: 20596704]

Author Manuscript Author Manuscript Author Manuscript Author Manuscript

110. Wai Y, et al. An integrated diffusion map for the analysis of diffusion properties: a feasibility study in patients with acoustic neuroma. Acad Radiol. 2009; 16(4):428–34. [PubMed: 19268854]

111. Nakayama T, et al. Use of diffusion-weighted MRI in monitoring response of lymph node metastatic bladder cancer treated with chemotherapy. Nihon Hinyokika Gakkai zasshi [Jpn J Urol]. 2008; 99(7):737–41.

112. Yoshida S, et al. Initial experience of diffusion-weighted magnetic resonance imaging to assess therapeutic response to induction chemoradiotherapy against muscle-invasive bladder cancer. Urology. 2010; 75(2):387–91. [PubMed: 19914691]

113. Ballon D, et al. Imaging therapeutic response in human bone marrow using rapid whole-body MRI. Magn Reson Med. 2004; 52(6):1234–8. [PubMed: 15562475]

114. Armitage PA, et al. Quantitative assessment of intracranial tumor response to dexamethasone using diffusion, perfusion and permeability magnetic resonance imaging. Magn Reson Imaging. 2007; 25(3):303–10. [PubMed: 17371718]

115. Bastin ME, et al. The use of diffusion tensor imaging in quantifying the effect of dexamethasone on brain tumours. Neuroreport. 1999; 10(7):1385–91. [PubMed: 10380951]

116. Huang CF, et al. Apparent diffusion coefficients for evaluation of the response of brain tumors treated by gamma knife surgery. J Neurosurg. 2010; 113(Suppl):97–104. [PubMed: 21222290]

117. Mardor Y, et al. Monitoring response to convection-enhanced taxol delivery in brain tumor patients using diffusion-weighted magnetic resonance imaging. Cancer Res. 2001; 61(13):4971–3. [PubMed: 11431326]

118. Mardor Y, et al. Pretreatment prediction of brain tumors' response to radiation therapy using high b-value diffusion-weighted MRI. Neoplasia. 2004; 6(2):136–42. [PubMed: 15140402]

119. Mardor Y, et al. Early detection of response to radiation therapy in patients with brain malignancies using conventional and high b-value diffusion-weighted magnetic resonance imaging. J Clin Oncol. 2003; 21(6):1094–100. [PubMed: 12637476]

120. Tomura N, et al. Diffusion changes in a tumor and peritumoral tissue after stereotactic irradiation for brain tumors: possible prediction of treatment response. J Comput Assist Tomogr. 2006; 30(3):496–500. [PubMed: 16778628]

121. Goldman M, et al. Utility of apparent diffusion coefficient in predicting the outcome of gamma knife-treated brain metastases prior to changes in tumor volume: a preliminary study. J Neurosurg. 2006; 105(Suppl):175–82. [PubMed: 18503353]

122. Gupta A, et al. Isolated diffusion restriction precedes the development of enhancing tumor in a subset of patients with glioblastoma. Am J Neuroradiol. 2011; 32(7):1301–6. [PubMed: 21596805]

123. Hattingen E, et al. Bevacizumab impairs oxidative energy metabolism and shows antitumoral effects in recurrent glioblastomas: a $^{31}P/^{1}H$ MRSI and quantitative magnetic resonance imaging study. Neuro-oncology. 2011; 13(12):1349–63. [PubMed: 21890539]

124. Pope WB, et al. Apparent diffusion coefficient histogram analysis stratifies progression-free survival in newly diagnosed bevacizumab-treated glioblastoma. Am J Neuroradiol. 2011; 32(5):882–9. [PubMed: 21330401]

125. Vrabec M, et al. MR perfusion and diffusion imaging in the follow-up of recurrent glioblastoma treated with dendritic cell immunotherapy: a pilot study. Neuroradiology. 2011; 53(10):721–31. [PubMed: 21107549]

126. Yamasaki F, et al. Advantages of high b-value diffusion-weighted imaging to diagnose pseudo-responses in patients with recurrent glioma after bevacizumab treatment. Eur J Radiol. 2012; 81(10):2805–10. [PubMed: 22100373]

127. Galban CJ, et al. Prospective analysis of parametric response map-derived MRI biomarkers: identification of early and distinct glioma response patterns not predicted by standard radiographic assessment. Clin Cancer Res. 2011; 17(14):4751–60. [PubMed: 21527563]

128. Nowosielski M, et al. ADC histograms predict response to anti-angiogenic therapy in patients with recurrent high-grade glioma. Neuroradiology. 2011; 53(4):291–302. [PubMed: 21125399]

129. Prabhu SP, et al. DTI assessment of the brainstem white matter tracts in pediatric BSG before and after therapy: a report from the Pediatric Brain Tumor Consortium. Child Nerv Syst. 2011; 27(1):11–8.

Author Manuscript Author Manuscript Author Manuscript Author Manuscript

130. Ringelstein A, et al. Evaluation of ADC mapping as an early predictor for tumor response to chemotherapy in recurrent glioma treated with bevacizumab/irinotecan: proof of principle. RoFo: Fortschr Gebiete Rontgenstrahlen Nuklearmedizin. 2010; 182(10):868–72.

131. Chen HJ, et al. Apparent diffusion and fractional anisotropy of diffuse intrinsic brain stem gliomas. Am J Neuroradiol. 2010; 31(10):1879–85. [PubMed: 20595371]

132. Jain R, et al. Imaging response criteria for recurrent gliomas treated with bevacizumab: role of diffusion weighted imaging as an imaging biomarker. J Neuro-oncol. 2010; 96(3):423–31.

133. Seshadri M, et al. MRI-based characterization of vascular disruption by 5,6-dimethylxanthenone-acetic acid in gliomas. J Cerebr Blood Flow Metab. 2009; 29(8):1373–82.

134. Jager HR, et al. Differential chemosensitivity of tumor components in a malignant oligodendroglioma: assessment with diffusion-weighted, perfusion-weighted, and serial volumetric MR imaging. Am J Neuroradiol. 2005; 26(2):274–8. [PubMed: 15709124]

135. Lidar Z, et al. Convection-enhanced delivery of paclitaxel for the treatment of recurrent malignant glioma: a phase I/II clinical study. J Neurosurg. 2004; 100(3):472–9. [PubMed: 15035283]

136. Lin YC, et al. Significant temporal evolution of diffusion anisotropy for evaluating early response to radiosurgery in patients with vestibular schwannoma: findings from functional diffusion maps. Am J Neuroradiol. 2010; 31(2):269–74. [PubMed: 19779002]

137. Schubert MI, et al. Diffusion-weighted magnetic resonance imaging of treatment-associated changes in recurrent and residual medulloblastoma: preliminary observations in three children. Acta Radiol. 2006; 47(10):1100–4. [PubMed: 17135017]

138. Sinha S, et al. Rapid clinical deterioration in a patient with multi-focal glioma despite corticosteroid therapy: a quantitative MRI study. Br J Neurosurg. 2003; 17(6):537–40. discussion 540. [PubMed: 14756481]

139. Arlinghaus LR, et al. On the relationship between the apparent diffusion coefficient and extravascular extracellular volume fraction in human breast cancer. Magn Reson Imaging. 2011; 29(5):630–8. [PubMed: 21531106]

140. Belli P, et al. Diffusion-weighted imaging in evaluating the response to neoadjuvant breast cancer treatment. Breast J. 2011; 17(6):610–9. [PubMed: 21929557]

141. Fangberget A, et al. Neoadjuvant chemotherapy in breast cancer-response evaluation and prediction of response to treatment using dynamic contrast-enhanced and diffusion-weighted MR imaging. Eur Radiol. 2011; 21(6):1188–99. [PubMed: 21127880]

142. Jensen LR, et al. Diffusion-weighted and dynamic contrast-enhanced MRI in evaluation of early treatment effects during neo-adjuvant chemotherapy in breast cancer patients. J Magn Reson Imaging. 2011; 34(5):1099–109. [PubMed: 22002757]

143. Jinming X, et al. Primary non-Hodgkin's lymphoma of the breast: mammography, ultrasound, MRI and pathologic findings. Future Oncol. 2012; 8(1):105–9. [PubMed: 22149038]

144. Kawamura M, et al. Early prediction of response to neoadjuvant chemotherapy for locally advanced breast cancer using MRI. Nagoya J Med Sci. 2011; 73(3–4):147–56. [PubMed: 21928696]

145. Li XR, et al. DW-MRI ADC values can predict treatment response in patients with locally advanced breast cancer undergoing neoadjuvant chemotherapy. Med Oncol. 2012; 29(2):425–31. [PubMed: 21286861]

146. Park SH, et al. Comparison of diffusion-weighted MR imaging and FDG PET/CT to predict pathological complete response to neoadjuvant chemotherapy in patients with breast cancer. Eur Radiol. 2012; 22(1):18–25. [PubMed: 21845462]

147. Wang XH, et al. Value of diffusion weighted imaging (DWI) in evaluating early response to neoadjuvant chemotherapy in locally advanced breast cancer. Zhonghua zhong liu za zhi [Chin J Oncol]. 2010; 32(5):377–81.

148. Buijs M, et al. Assessment of metastatic breast cancer response to chemoembolization with contrast agent enhanced and diffusion-weighted MR imaging. J Vasc Intervent Radiol. 2007; 18(8):957–63.

149. Ma B, et al. Voxel-by-voxel functional diffusion mapping for early evaluation of breast cancer treatment. Proc Conf Inform Process Med Imaging. 2009; 21:276–87.

150. Nilsen L, et al. Diffusion-weighted magnetic resonance imaging for pretreatment prediction and monitoring of treatment response of patients with locally advanced breast cancer undergoing neoadjuvant chemotherapy. Acta Oncol. 2010; 49(3):354–60. [PubMed: 20397769]

151. Tozaki M, et al. Preliminary study of early response to neoadjuvant chemotherapy after the first cycle in breast cancer: comparison of ^{1}H magnetic resonance spectroscopy with diffusion magnetic resonance imaging. Jpn J Radiol. 2010; 28(2):101–9. [PubMed: 20182844]

152. Manton DJ, et al. Neoadjuvant chemotherapy in breast cancer: early response prediction with quantitative MR imaging and spectroscopy. Br J Cancer. 2006; 94(3):427–35. [PubMed: 16465174]

153. Harry VN, et al. Diffusion-weighted magnetic resonance imaging in the early detection of response to chemoradiation in cervical cancer. Gynecol Oncol. 2008; 111(2):213–20. [PubMed: 18774597]

154. Levy A, et al. Accuracy of diffusion-weighted echo-planar MR imaging and ADC mapping in the evaluation of residual cervical carcinoma after radiation therapy. Gynecol Oncol. 2011; 123(1): 110–5. [PubMed: 21764110]

155. Liu Y, et al. Diffusion-weighted imaging in predicting and monitoring the response of uterine cervical cancer to combined chemoradiation. Clin Radiol. 2009; 64(11):1067–74. [PubMed: 19822239]

156. Matge G. Anterior interbody fusion with the BAK-cage in cervical spondylosis. Acta Neurochirurg. 1998; 140(1):1–8.

157. McVeigh PZ, et al. Diffusion-weighted MRI in cervical cancer. Eur Radiol. 2008; 18(5):1058–64. [PubMed: 18193428]

158. Rizzo S, et al. Diffusion-weighted MR imaging in assessing cervical tumour response to nonsurgical therapy. Radiol Med. 2011; 116(5):766–80. [PubMed: 21424319]

159. Zhang Y, et al. Diffusion-weighted magnetic resonance imaging for prediction of response of advanced cervical cancer to chemoradiation. J Comput Assist Tomogr. 2011; 35(1):102–7. [PubMed: 21245694]

160. Zhang Y, et al. Diffusion weighted imaging features of normal uterine cervix and cervical carcinoma. Ai zheng = Aizheng [Chin J Cancer]. 2007; 26(5):508–12.

161. Buijs M, et al. Chemoembolization of hepatic metastases from ocular melanoma: assessment of response with contrast-enhanced and diffusion-weighted MRI. Am J Roentgenol. 2008; 191(1): 285–9. [PubMed: 18562760]

162. Politi LS, et al. Ocular adnexal lymphoma: diffusion-weighted MR imaging for differential diagnosis and therapeutic monitoring. Radiology. 2010; 256(2):565–74. [PubMed: 20656841]

163. Hecht EM, et al. Diffusion-weighted imaging for prediction of volumetric response of leiomyomas following uterine artery embolization: a preliminary study. J Magn Reson Imaging. 2011; 33(3):641–6. [PubMed: 21563247]

164. Saraiya B, et al. Phase I study of gemcitabine, docetaxel and imatinib in refractory and relapsed solid tumors. Invest New Drugs. 2012; 30(1):258–65. [PubMed: 20697775]

165. Vossen JA, et al. Role of functional magnetic resonance imaging in assessing metastatic leiomyosarcoma response to chemoembolization. J Comput Assist Tomogr. 2008; 32(3):347–52. [PubMed: 18520535]

166. Choi SA, et al. The effect of gadoxetic acid enhancement on lesion detection and characterisation using T(2) weighted imaging and diffusion weighted imaging of the liver. Br J Radiol. 2012; 85(1009):29–36. [PubMed: 21123305]

167. Dudeck O, et al. Early prediction of anticancer effects with diffusion-weighted MR imaging in patients with colorectal liver metastases following selective internal radiotherapy. Eur Radiol. 2010; 20(11):2699–706. [PubMed: 20563725]

168. Koh DM, et al. Predicting response of colorectal hepatic metastasis: value of pretreatment apparent diffusion coefficients. Am J Roentgenol. 2007; 188(4):1001–8. [PubMed: 17377036]

169. Wybranski C, et al. Value of diffusion weighted MR imaging as an early surrogate parameter for evaluation of tumor response to high-dose-rate brachytherapy of colorectal liver metastases. Radiat Oncol. 2011; 6(1):43. [PubMed: 21524305]

Author Manuscript Author Manuscript Author Manuscript Author Manuscript

Author Manuscript Author Manuscript Author Manuscript Author Manuscript

170. Zhang Y, et al. Evaluation of short-term response of high intensity focused ultrasound ablation for primary hepatic carcinoma: utility of contrast-enhanced MRI and diffusion-weighted imaging. Eur J Radiol. 2011; 79(3):347–52. [PubMed: 20638211]
171. Duke E, et al. Agreement between competing imaging measures of response of hepatocellular carcinoma to yttrium-90 radioembolization. J Vasc Intervent Radiol. 2010; 21(4):515–21.
172. Kubota K, et al. Role of diffusion-weighted imaging in evaluating therapeutic efficacy after transcatheter arterial chemoembolization for hepatocellular carcinoma. Oncol Rep. 2010; 24(3): 727–32. [PubMed: 20664980]
173. Liapi E, et al. Functional MRI evaluation of tumor response in patients with neuroendocrine hepatic metastasis treated with trans-catheter arterial chemoembolization. Am J Roentgenol. 2008; 190(1):67–73. [PubMed: 18094295]
174. Eccles CL, et al. Change in diffusion weighted MRI during liver cancer radiotherapy: preliminary observations. Acta Oncol. 2009; 48(7):1034–43. [PubMed: 19634060]
175. Schraml C, et al. Diffusion-weighted MRI of advanced hepatocellular carcinoma during sorafenib treatment: initial results. Am J Roentgenol. 2009; 193(4):W301–7. [PubMed: 19770299]
176. Yuan Z, et al. Role of magnetic resonance diffusion-weighted imaging in evaluating response after chemoembolization of hepatocellular carcinoma. Eur J Radiol. 2010; 75(1):e9–e14. [PubMed: 19540083]
177. Anzidei M, et al. Liver metastases from colorectal cancer treated with conventional and antiangiogenetic chemotherapy: evaluation with liver computed tomography perfusion and magnetic resonance diffusion-weighted imaging. J Comput Assist Tomogr. 2011; 35(6):690–6. [PubMed: 22082538]
178. Bonekamp S, et al. Early response of hepatic malignancies to locoregional therapy – value of diffusion-weighted magnetic resonance imaging and proton magnetic resonance spectroscopy. J Comput Assist Tomogr. 2011; 35(2):167–73. [PubMed: 21412085]
179. Yuan Z, et al. Water mobility of diffusion MRI in prediction of response to chemoembolization in liver cancer. Zhonghua zhong liu za zhi [Chin J Oncol]. 2009; 31(4):293–7.
180. Chung JC, et al. Diffusion-weighted magnetic resonance imaging to predict response of hepatocellular carcinoma to chemoembolization. World J Gastroenterol. 2010; 16(25):3161–7. [PubMed: 20593501]
181. El-Khouli RH, et al. Solitary fibrous tumor of the liver: magnetic resonance imaging evaluation and treatment with transarterial chemoembolization. J Comput Assist Tomogr. 2008; 32(5):769–71. [PubMed: 18830108]
182. Chang Q, et al. Diffusion-weighted magnetic resonance imaging of lung cancer at 3.0 T: a preliminary study on monitoring diffusion changes during chemoradiation therapy. Clin Imaging. 2012; 36(2):98–103. [PubMed: 22370130]
183. Ohno Y, et al. Diffusion-weighted MRI versus ^{18}F-FDG PET/CT: performance as predictors of tumor treatment response and patient survival in patients with non-small cell lung cancer receiving chemoradiotherapy. Am J Roentgenol. 2012; 198(1):75–82. [PubMed: 22194481]
184. Okuma T, et al. Assessment of early treatment response after CT-guided radiofrequency ablation of unresectable lung tumours by diffusion-weighted MRI: a pilot study. Br J Radiol. 2009; 82(984):989–94. [PubMed: 19470575]
185. Zhou R, et al. Diffusion-weighted imaging for assessment of lung cancer response to chemotherapy. Zhongguo fei ai za zhi [Chin J Lung Cancer]. 2011; 14(3):256–60.
186. Lin C, et al. Whole-body diffusion-weighted imaging with apparent diffusion coefficient mapping for treatment response assessment in patients with diffuse large B-cell lymphoma: pilot study. Invest Radiol. 2011; 46(5):341–9. [PubMed: 21263330]
187. Marzolini M, et al. Diffusion-weighted MRI compared to FDG PET-CT in the staging and response assessment of Hodgkin lymphoma. Br J Haematol. 2012; 156(5):557. [PubMed: 22150023]
188. Wu X, et al. Diffusion-weighted MRI in early chemotherapy response evaluation of patients with diffuse large B-cell lymphoma —a pilot study: comparison with 2-deoxy-2-fluoro-D-glucose-positron emission tomography/computed tomography. NMR Biomed. 2011; 24(10):1181–90. [PubMed: 21387451]

Author Manuscript Author Manuscript Author Manuscript Author Manuscript

189. Fenchel M, et al. Response assessment in patients with multiple myeloma during antiangiogenic therapy using arterial spin labeling and diffusion-weighted imaging: a feasibility study. Acad Radiol. 2010; 17(11):1326–33. [PubMed: 20817572]

190. Horger M, et al. Whole-body diffusion-weighted MRI with apparent diffusion coefficient mapping for early response monitoring in multiple myeloma: preliminary results. Am J Roentgenol. 2011; 196(6):W790–5. [PubMed: 21606271]

191. Kyriazi S, et al. Metastatic ovarian and primary peritoneal cancer: assessing chemotherapy response with diffusion-weighted MR imaging—value of histogram analysis of apparent diffusion coefficients. Radiology. 2011; 261(1):182–92. [PubMed: 21828186]

192. Kyriazi S, et al. Value of diffusion-weighted imaging for assessing site-specific response of advanced ovarian cancer to neoadjuvant chemotherapy: correlation of apparent diffusion coefficients with epithelial and stromal densities on histology. Cancer Biomarkers Sect A: Disease Markers. 2010; 7(4):201–10.

193. Sala E, et al. Advanced ovarian cancer: multiparametric MR imaging demonstrates response- and metastasis-specific effects. Radiology. 2012; 263(1):149–59. [PubMed: 22332064]

194. Niwa T, et al. Advanced pancreatic cancer: the use of the apparent diffusion coefficient to predict response to chemotherapy. Br J Radiol. 2009; 82(973):28–34. [PubMed: 19095814]

195. Barrett T, et al. DCE and DW MRI in monitoring response to androgen deprivation therapy in patients with prostate cancer: a feasibility study. Magn Reson Med. 2012; 67(3):778–85. [PubMed: 22135228]

196. Messiou C, et al. Assessing response in bone metastases in prostate cancer with diffusion weighted MRI. Eur Radiol. 2011; 21(10):2169–77. [PubMed: 21710270]

197. Nemoto K, et al. Changes in diffusion-weighted images for visualizing prostate cancer during antiandrogen therapy: preliminary results. Urol Int. 2010; 85(4):421–6. [PubMed: 21051871]

198. Song I, et al. Assessment of response to radiotherapy for prostate cancer: value of diffusion-weighted MRI at 3 T. Am J Roentgenol. 2010; 194(6):W477–82. [PubMed: 20489065]

199. Curvo-Semedo L, et al. Rectal cancer: assessment of complete response to preoperative combined radiation therapy with chemotherapy—conventional MR volumetry versus diffusion-weighted MR imaging. Radiology. 2011; 260(3):734–43. [PubMed: 21673229]

200. Jang KM, et al. Pathological correlation with diffusion restriction on diffusion-weighted imaging in patients with pathological complete response after neoadjuvant chemoradiation therapy for locally advanced rectal cancer: preliminary results. Br J Radiol. 2012; 85(1017):e566–72. [PubMed: 22422387]

201. Kim SH, et al. Apparent diffusion coefficient for evaluating tumour response to neoadjuvant chemoradiation therapy for locally advanced rectal cancer. Eur Radiol. 2011; 21(5):987–95. [PubMed: 20978768]

202. Lambrecht M, et al. Value of diffusion-weighted magnetic resonance imaging for prediction and early assessment of response to neoadjuvant radiochemotherapy in rectal cancer: preliminary results. Int J Radiat Oncol Biol Phys. 2012; 82(2):863–70. [PubMed: 21398048]

203. Lambregts DM, et al. Tumour ADC measurements in rectal cancer: effect of ROI methods on ADC values and interobserver variability. Eur Radiol. 2011; 21(12):2567–74. [PubMed: 21822946]

204. Lambregts DM, et al. Diffusion-weighted MRI for selection of complete responders after chemoradiation for locally advanced rectal cancer: a multicenter study. Ann Surg Oncol. 2011; 18(8):2224–31. [PubMed: 21347783]

205. Seehaus A, et al. Diffusion-weighted MR imaging in patients with rectal cancer: our initial experience. Acta Gastroenterol Latinoam. 2011; 41(3):199–207. [PubMed: 22232997]

206. DeVries AF, et al. Tumor microcirculation and diffusion predict therapy outcome for primary rectal carcinoma. Int J Radiat Oncol Biol Phys. 2003; 56(4):958–65. [PubMed: 12829130]

207. Lambrecht M, et al. The use of FDG-PET/CT and diffusion-weighted magnetic resonance imaging for response prediction before, during and after preoperative chemoradiotherapy for rectal cancer. Acta Oncol. 2010; 49(7):956–63. [PubMed: 20586658]

Author Manuscript Author Manuscript Author Manuscript Author Manuscript

208. Bajpai J, et al. Role of MRI in osteosarcoma for evaluation and prediction of chemotherapy response: correlation with histological necrosis. Pediatr Radiol. 2011; 41(4):441–50. [PubMed: 20978754]

209. Baunin C, et al. Value of diffusion-weighted images in differentiating mid-course responders to chemotherapy for osteosarcoma compared to the histological response: preliminary results. Skel Radiol. 2012; 41(9):1141–9.

210. Dudeck O, et al. Diffusion-weighted magnetic resonance imaging allows monitoring of anticancer treatment effects in patients with soft-tissue sarcomas. J Magn Reson Imaging. 2008; 27(5): 1109–13. [PubMed: 18425832]

211. Oka K, et al. The value of diffusion-weighted imaging for monitoring the chemotherapeutic response of osteosarcoma: a comparison between average apparent diffusion coefficient and minimum apparent diffusion coefficient. Skel Radiol. 2010; 39(2):141–6.

212. Uhl M, et al. Evaluation of tumour necrosis during chemotherapy with diffusion-weighted MR imaging: preliminary results in osteosarcomas. Pediatr Radiol. 2006; 36(12):1306–11. [PubMed: 17031633]

213. Einarsdottir H, et al. Diffusion-weighted MRI of soft tissue tumours. Eur Radiol. 2004; 14(6): 959–63. [PubMed: 14767604]

214. Koh DM, et al. Reproducibility and changes in the apparent diffusion coefficients of solid tumours treated with combretastatin A4 phosphate and bevacizumab in a two-centre phase I clinical trial. Eur Radiol. 2009; 19(11):2728–38. [PubMed: 19547986]

215. Dirix P, et al. Dose painting in radiotherapy for head and neck squamous cell carcinoma: value of repeated functional imaging with (18)F-FDG PET, (18)F-fluoromisonidazole PET, diffusion-weighted MRI, and dynamic contrast-enhanced MRI. J Nucl Med. 2009; 50(7):1020–7. [PubMed: 19525447]

216. King AD, et al. Squamous cell carcinoma of the head and neck: diffusion-weighted MR imaging for prediction and monitoring of treatment response. Eur Radiol. 2010; 20(9):2213–20. [PubMed: 20309553]

217. Vandecaveye V, et al. Predictive value of diffusion-weighted magnetic resonance imaging during chemoradiotherapy for head and neck squamous cell carcinoma. Eur Radiol. 2010; 20(7):1703–14. [PubMed: 20179939]

218. Vandecaveye V, et al. Diffusion-weighted magnetic resonance imaging early after chemoradiotherapy to monitor treatment response in head-and-neck squamous cell carcinoma. Int J Radiat Oncol Biol Phys. 2012; 82(3):1098–107. [PubMed: 21514067]

219. Kato H, et al. Head and neck squamous cell carcinoma: usefulness of diffusion-weighted MR imaging in the prediction of a neoadjuvant therapeutic effect. Eur Radiol. 2009; 19(1):103–9. [PubMed: 18641991]

220. Kim S, et al. Diffusion-weighted magnetic resonance imaging for predicting and detecting early response to chemoradiation therapy of squamous cell carcinomas of the head and neck. Clin Cancer Res. 2009; 15(3):986–94. [PubMed: 19188170]

Author Manuscript
Author Manuscript
Author Manuscript
Author Manuscript

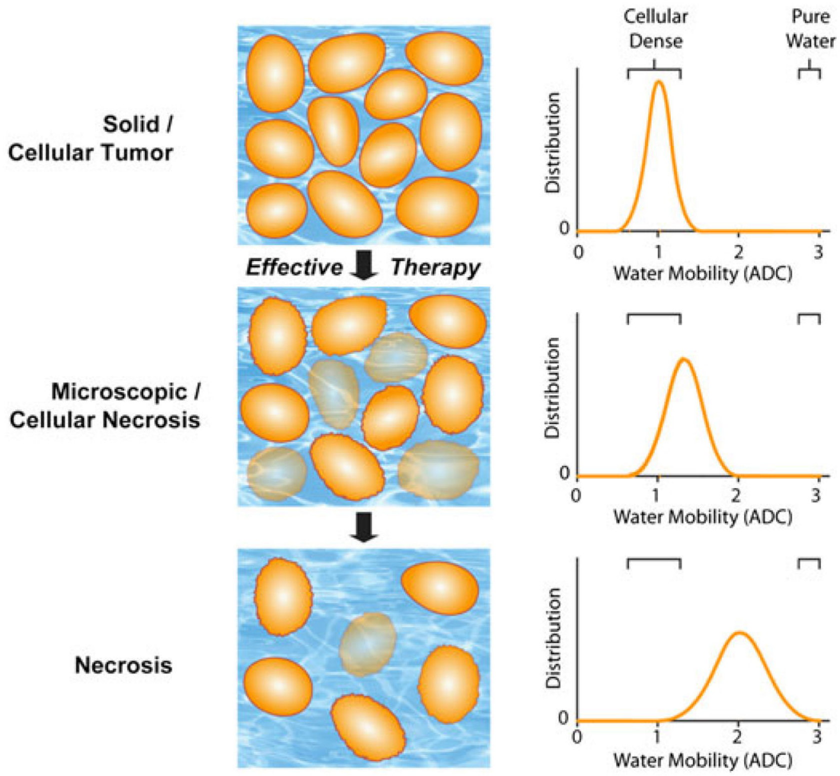

Figure 1.
Schematic diagram of changes in water diffusivity in a tumor following an effective therapeutic agent. Changes in cellularity (left) occur with increasing molecular water mobility, measured as the apparent diffusion coefficient (ADC; right), as a tumor responds to treatment (top to bottom). As a tumor responds to therapy, an increase in extracellular space and membrane permeability occurs, which allows for increased water mobility, and is detected by diffusion-weighted MRI (DW-MRI) as an increase in ADC values. [Courtesy of ref. (18).]

Author Manuscript Author Manuscript Author Manuscript Author Manuscript

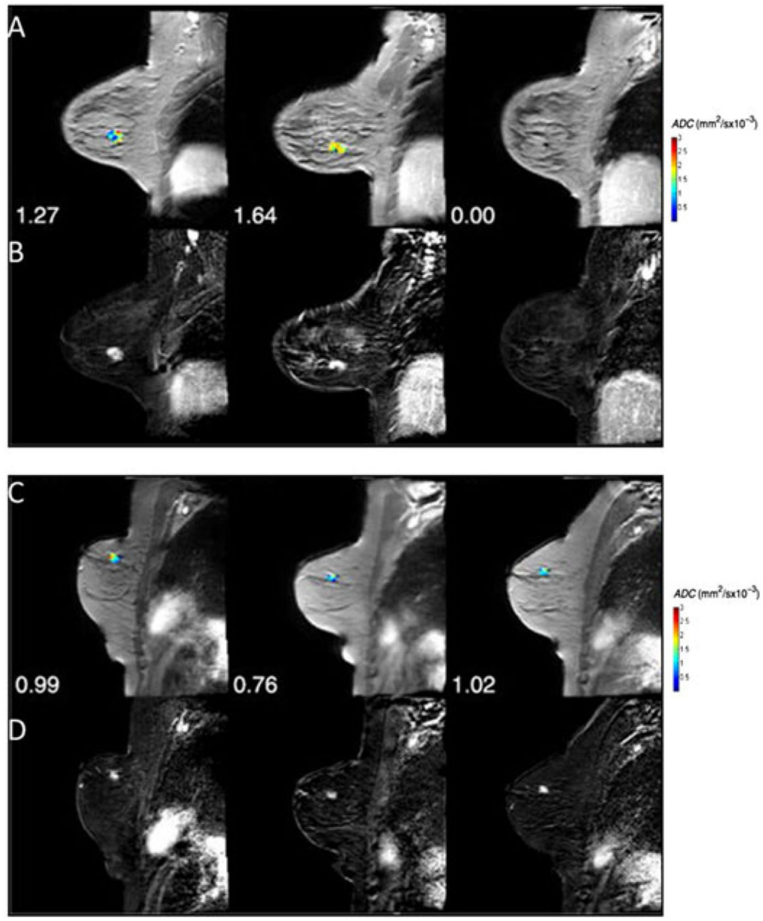

Figure 2.

(A) Apparent diffusion coefficient (ADC) maps superimposed on the post-contrast dynamic contrast-enhanced MR (DCE-MR) images at three time points [pre-treatment, after one cycle and after all cycles of neoadjuvant chemotherapy (NAC)] for a patient achieving pathological complete response (pCR). The numbers for each panel represent the mean ADC values for each time point in the parametric map. (B) The difference image between pre-contrast and post-contrast DCE-MRI at each time point. (C) ADC maps superimposed on the post-contrast DCE-MR images at three time points (pre-treatment, after one cycle and after all cycles of NAC) for a non-pCR patient. The numbers for each panel represent the mean ADC values for each time point in the parametric map. (D) The difference image between pre-contrast and post-contrast DCE-MRI at each time point. [Courtesy of and adapted from ref. (73).]

Author Manuscript
Author Manuscript
Author Manuscript
Author Manuscript

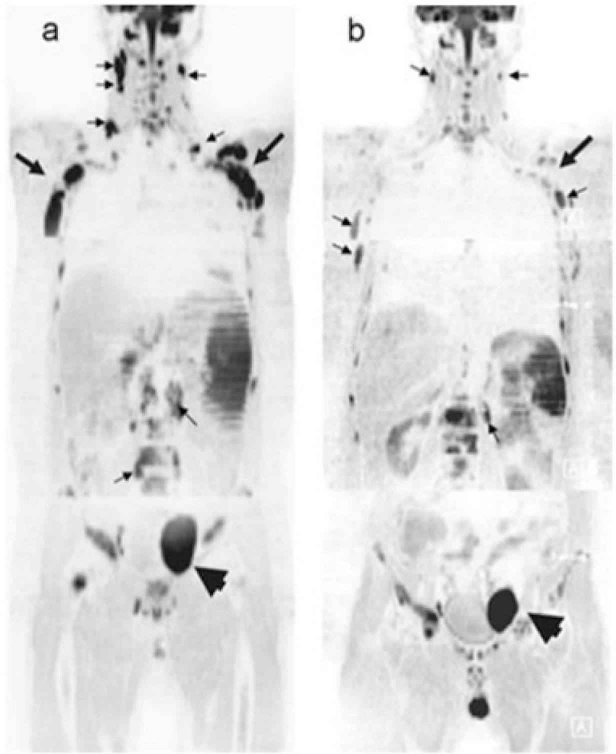

Figure 3.

Whole-body diffusion-weighted MRI (wbDW-MRI) is presented as an early indicator of response to systemic therapy in patients with lymphoma. (A) Image of a 48-year-old man diagnosed with diffuse large B-cell lymphoma obtained at baseline shows the ubiquitous involvement of lymph nodes (e.g. cervical and retroperitoneal, small arrows) and axillary regions (large arrows) with marked restriction of water diffusivity. A larger pelvic node (arrowhead) is also seen left of the midline. (B) At day 7 following the institution of chemotherapy with rituximab (anti-CD20 antibodies) + CHOP (cyclophosphamide, hydroxydaunorubicin, vincristine, prednisolone), wbDW-MRI shows evident reduction in signal intensity in the cervical and retroperitoneal node regions (small arrows) and axillary region (large arrows) (from ADC = 0.90/0.33/0.67/0.61 to ADC = 1.66/0.73/1.36/1.22), with a corresponding increase in ADC (not shown), but a less marked response, in the pelvic node (arrowhead) (from ADC = 0.83/0.51 to ADC = 1.12/0.67) At the interim, the patient achieved complete remission. [Courtesy of ref. (59).]

Author Manuscript
Author Manuscript
Author Manuscript
Author Manuscript

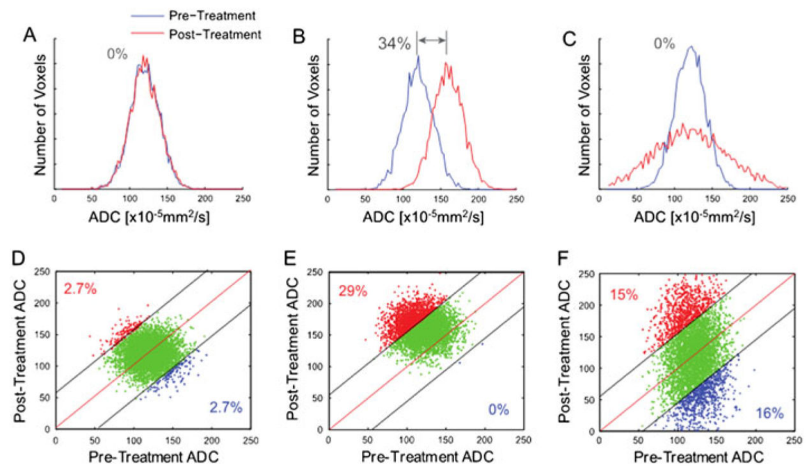

Figure 4.

Simulated comparison of whole-tumor histogram analysis (top row; blue line, pre-treatment tumor data; red line, post-treatment tumor data) *versus* the corresponding voxel-based analysis using a joint density histogram (bottom row). Histograms from tumors with no major change (A), significant uniform shift to higher apparent diffusion coefficient (ADC) values with a 34% net mean change (B) and heterogeneous ADC changes (increased and decreased ADC values) resulting in no net detectable histogram shift (C). Parametric response maps from the corresponding histograms are also shown, where, in (D), the confidence interval for the detection of change was set to 95%, and thus no significant change in red voxels (increased values) or blue voxels (decreased values) was detected. (E) An increase in the number of red voxels was detected at 29% of the total tumor voxels. (F) Both an increase and a decrease in tumor voxels of approximately 15% were detected, whereas no major shift was detected using a histogram analysis of the same data (C). [Courtesy of Ref. (85).]

Author Manuscript Author Manuscript Author Manuscript Author Manuscript

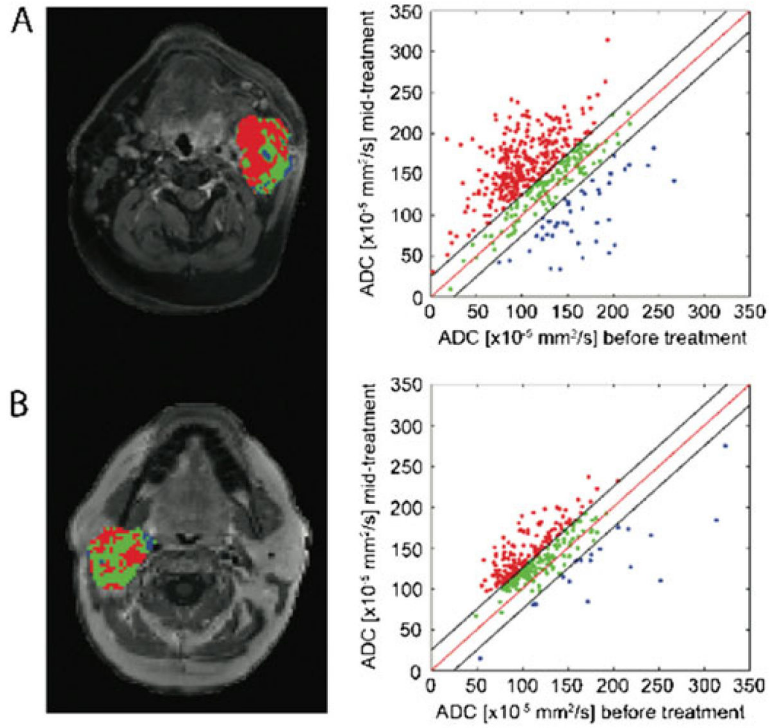

Figure 5.

Functional diffusion mapping (fDM) applied to clinical data acquired from patients with head and neck squamous cell carcinoma (HNSCC) diagnosed as pCR (pathological complete response) (A) and PR (partial response) (B). Results from the fDM analysis are presented as color-coded maps superimposed on contrast-enhanced T_1-weighted images and scatter plots with axes pre-treatment ADC (*x*-axis) and post-treatment ADC (*y*-axis). Color-coding is as follows: red, increased ADC values; blue, decreased ADC values; green, unchanged ADC values. [Courtesy of ref. (65).]

Author Manuscript Author Manuscript Author Manuscript Author Manuscript

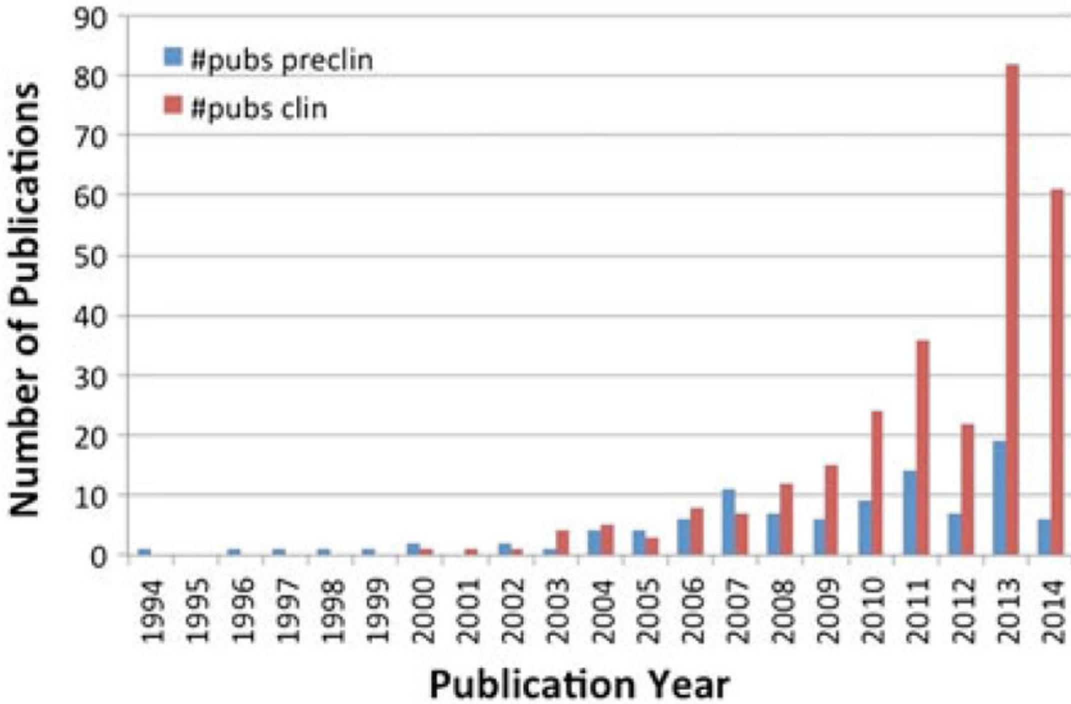

Figure 6.

Number of annual publications on the application of diffusion-weighted MRI (DW-MRI) for therapeutic response assessment. Yearly evaluation showed a growing increase in the number of studies demonstrating the efficacy of DW-MRI for cancer response to treatment. The search was performed on Pubmed using the following criteria [((diffusion OR ADC OR "apparent diffusion coefficient") AND MRI AND response) NOT (stroke OR review)]. Individual references were manually evaluated.

Author Manuscript Author Manuscript Author Manuscript Author Manuscript

Table 1

Please provide legend

Site	Reference
Abdominal	(109)
Acoustic neuroma	(110)
Bladder	(111,112)
Bone marrow	(113)
Brain	(26,87,93,114–138)
Breast	(35–38,139–152)
Cervical	(153–160)
Eye	(161,162)
Leiomyoma	(163–165)
Liver	(41,42,44,46,70,166–181)
Lung	(182–185)
Lymphoma	(186–188)
Myeloma	(189,190)
Ovarian	(191–193)
Pancreas	(194)
Prostate	(29,195–198)
Rectal	(54,79,199–207)
Sarcoma	(208–214)
HNSCC	(65,215–220)

[1]HNSCC, head and neck squamous cell carcinoma.